DMD Fast Forward. Published on December 15, 2008 as doi:10.1124/dmd.108.025171

Novel Metabolites of Amodiaquine Formed by CYP1A1 and CYP1B1 – Structure Elucidation using Electrochemistry, MS and NMR

Tove Johansson, Ulrik Jurva, Gunnar Grönberg, Lars Weidolf, Collen Masimirembwa

Discovery DMPK & Bioanalytical Chemistry, AstraZeneca R&D Mölndal, Sweden (T.J.), Department of Chemistry, Medicinal Chemistry, University of Gothenburg, Göteborg, Sweden (T.J.), Lead Generation, AstraZeneca R&D Mölndal, Sweden (U.J.), Medicinal Chemistry, AstraZeneca R&D Mölndal, Sweden (G.G.), Clinical Pharmacology & DMPK, AstraZeneca R&D Mölndal, Sweden (L.W.), Department of DMPK/PD & Toxicology, African Institute of Biomedical Science & Technology (AiBST), Harare, Zimbabwe (C.M.)

DMD Fast Forward. Published on December 15, 2008 as DOI: 10.1124/dmd.108.025171

Running title:

Novel Metabolites of Amodiaquine Formed by CYP1A1 and CYP1B1

Corresponding author:

Tove Johansson, Discovery DMPK & Bioanalytical Chemistry, AstraZeneca R&D Mölndal, SE-431 83 Mölndal, Sweden.

Tel.: +46 31 7065006

Fax: +46 31 7763867

Email: tove.e.johansson@astrazeneca.com

Number of text pages: 25 (including references, tables and figure texts)

Tables: 2

Figures: 6

References: 32

Word counts:

Abstract: 215

Introduction: 750

Discussion: 1004

[1] Abbreviations used are:
EC-ESI/MS, electrochemistry online with electrospray mass spectrometry; *m/z*, mass-to-charge ratio; HLM, human rat liver microsomes; RLM, rat liver microsomes; EROD, ethoxyresorufin *O*-deethylation; COSY, correlation spectroscopy; NOE, nuclear Overhauser effect; s, singlet; d, doublet; br, broad; t, triplet; NAC, *N*-acetyl cysteine; MA, methoxyl amine; SPE, solid phase extraction; CYP, cytochrome P450; rCYP, recombinantly expressed CYP; TCI, triple-resonance inverse cryoprobe; HSQC, heteronuclear single quantum coherence

DMD Fast Forward. Published on December 15, 2008 as DOI: 10.1124/dmd.108.025171

Abstract

An aldehyde metabolite of amodiaquine and desethylamodiaquine has been identified. The aldehyde was the major metabolite formed in incubations with two recombinantly expressed human CYPs (rCYPs), namely CYP1A1 and CYP1B1. The aldehyde metabolite was also formed, to a lesser extent, in both human and rat liver microsomes. When comparing results from incubations with liver microsomes from 3-methylcholanthrene-treated rats (inducing CYP1A1 and CYP1B1) with those from non-induced rats, a 6-fold increase of the aldehyde metabolite was observed in the rat liver microsomes after 3-methylcholanthrene treatment. The metabolic oxidation was mimicked by the electrochemical system and the electrochemical oxidation product was matched with the metabolite from the in vitro incubations. The electrochemical generation of the aldehyde metabolite was repeated on a preparative scale and the proposed structure was confirmed by NMR. Trapping of the aldehyde metabolite was done with methoxyl amine. Trapping experiments with *N*-acetyl cysteine revealed that the aldehyde was further oxidized to an aldehyde quinoneimine species, both in the rCYP incubations and in the electrochemical system. Three additional new metabolites of amodiaquine and desethylamodiaquine were formed via rCYP1A1 and rCYP1B1. Trace amounts of these metabolites were also observed in incubations with liver microsomes from 3-methylcholanthrene treated rats. Tentative structures of the metabolites and adducts were assigned based on LC/MS/MS in combination with accurate mass measurements.

DMD Fast Forward. Published on December 15, 2008 as DOI: 10.1124/dmd.108.025171

Introduction

Amodiaquine **1** was discovered in the 1950s as an effective antimalarial drug (Mein, 1951). It was withdrawn from clinical use in the 1970s due to its toxicity. The drug is, however, gaining wide-spread use in Africa and Asia where chloroquine resistance is on the increase (Pussard et al., 1987). Because of severe side-effects including hepatitis and agranulocytosis observed during prophylactic use of the drug, **1** is now only used for the treatment of the acute phase of malaria, during which, no serious cases of toxicity have been reported (Laurent et al., 1993). It is administered in combination with other antimalarials such as artesunate in the artemisinin based combination therapy currently recommended by WHO (Durrani et al., 2005).

Earlier studies have identified a quinoneimine metabolite as the likely cause of amodiaquine toxicity through various actions. The biochemical basis of the toxicity of **1** has been explored in depth by the group of Park as possibly being due to the reactivity of the quinoneimine group (Maggs et al., 1988; Christie et al., 1989; Clarke et al., 1990; Clarke et al., 1991; Harrison et al., 1992; Jewell et al., 1995; Naisbitt et al., 1998).

1 is rapidly absorbed and extensively metabolized after oral administration to humans resulting in low plasma exposure of the parent drug (Laurent et al., 1993). Desethylamodiaquine **2** is the main metabolite of **1**, and other reported metabolites are bisdesethylamodiaquine and 2-hydroxydesethylamodiaquine (Churchill et al., 1985; Mount et al., 1986). **1** is rapidly converted to **2** whereas the elimination of **2** is very slow with a long terminal half-life (Pussard et al., 1987; Laurent et al., 1993). Both parent and metabolite have antimalarial activity making the parent **1** act like a prodrug to the metabolite **2** (Churchill et al., 1985). In studies to identify the enzymes responsible for the metabolism of **1** to **2**, it was found that CYP2C8 was the main enzyme responsible for this reaction (Li et al., 2002; Li et al., 2003).

On screening a panel of 13 human rCYPs, in addition to the finding that CYP2C8 was mainly responsible for the elimination of **1** and the formation of **2**, it was also found that CYP1A1 and CYP1B1

mediated the formation of an unidentified metabolite, M2. This metabolite was not observed in incubations with human liver microsomes (Li et al., 2002; Li et al., 2003). This may be explained by the fact that CYP1A1 and CYP1B1 mainly are found in extrahepatic tissues. However, these two enzymes are expressed in low levels in human liver (Hakkola et al., 1997; Stiborova et al., 2002; Stiborova et al., 2005) and at least CYP1A1 is expressed in low levels in rat liver (Harrigan et al., 2006; Stiborova et al., 2006). Previous studies have shown that 3-methylcholanthrene induces CYP1A1 and CYP1B1 in rat liver (Caron et al., 2005) and also CYP1A1 in human hepatocytes (Bowen et al., 2000). CYP1A1 and CYP1B1 are involved in the bioactivation of many procarcinogens (Shimada et al., 2001) and induced by a series of polyaromatic hydrocarbons (Pushparajah et al., 2008). Thus it is of interest to establish the structure of M2 and assess its potential reactivity.

The EC/ESI-MS technique combines electrochemistry (EC) online with electrospray ionisation mass spectrometry (ESI-MS) (Zhou and Van Berkel, 1995). Electrochemistry has been shown to be a useful means to mimic oxidative drug metabolism, including oxidation to reactive metabolites (Johansson et al., 2007; Lohmann and Karst, 2007; Madsen et al., 2007; Jurva et al., 2008). A previous publication presents a thorough study on which phase I drug metabolism reactions the EC system is able to mimic, including discussion on advantages and disadvantages of the technique (Johansson et al., 2007). In a study to demonstrate the utility of EC oxidation for generating electrophilic drug metabolites for characterization, **1** was investigated. In addition to the formation of the quinoneimine species of **1** another electrochemical oxidation product of **1** was also generated for which an aldehyde structure was proposed (Jurva et al., 2008). The molecular mass of this oxidation product turned out to be the same as that of the unidentified metabolite M2, which was discovered in the previous metabolism study with CYP1A1 and CYP1B1 (Li et al., 2002; Jurva et al., 2008). Another research group has also proposed an aldehyde structure for an electrochemical oxidation product of **1** (Lohmann and Karst, 2007).

The aim of this present study was to identify and chemically characterize M2 (in this study called **3**) using in vitro systems and electrochemical oxidation techniques. Structures **1**-**3** are presented in Fig. 1.

DMD Fast Forward. Published on December 15, 2008 as DOI: 10.1124/dmd.108.025171

Methods

Chemicals. The following chemicals were obtained commercially: amodiaquine (**1**) dihydrochloride dihydrate, Sigma; 7-ethoxyresorufin, Invitrogen; methoxyl amine hydrochloride, 98%, Sigma; β-NADPH, reduced form tetrasodium salt, 98%, Sigma; leucine enkephalin acetate hydrate, 97%, Sigma; *N*-α-acetyl-L-lysine, Sigma; *N*-acetyl-L-cysteine, >99%, Sigma; deuterated acetonitrile, 99.96% D, Armar Chemicals; desethylamodiaquine (**2**) dihydrochloride, 98.25%, LGC GmbH; methanol, Rathburn Chemicals; formic acid, 98-100%, Merck; acetonitrile, Fischer Scientific. All solvents were of analytical grade and the water used in the experiments was obtained from a water purification system (Elgastat Maxima, ELGA, Lane End, UK).

Incubations with rCYPs. The source of recombinant enzymes was bacterial membranes containing human cytochrome P450 (CYP1A1, CYP1B1 and CYP2J2) coexpressed with NADPH-cytochrome P450 reductase purchased from Cypex Ltd. (Scotland, UK). The incubation mixture, containing 100 pmol/ml of enzyme and 5 μM amodiaquine **1** or desethylamodiaquine **2** in 0.1 M phosphate buffer (pH 7.4) were pre-incubated for 5 minutes at 37°C. Methoxyl amine (dissolved in water) was added to a final concentration of 5 mM to trap the aldehyde metabolite **3** and *N*-acetyl cysteine (dissolved in water) was added to a final concentration of 5 mM for trapping the quinoneimines. The reaction was initiated by adding NADPH to a final concentration of 1 mM and the reaction mixtures (final volume 150 μl) were incubated for 30 minutes at 37°C. Control incubations were conducted in the absence of NADPH and in the absence of substrate. The reactions were quenched by adding 150 μl ice-cold acetonitrile. The samples were vortexed for 10 seconds and then centrifuged for 10 minutes at +4°C, 4000 rpm (~ 2750g). All incubations were performed in duplicate. The supernatants were stored at -18°C until analysis.

Incubations with liver microsomes. Human liver microsomes (HLM) were purchased from BD Biosciences (Woburn, MA, USA). Rat liver microsomes (non-induced and from 3-methylcholanthrene treated rats) were from male Sprague-Dawley rats and were purchased from In Vitro Technologies. 3-methylcholanthrene induces CYP1A1 and CYP1B1 in rat (Caron et al., 2005). The incubation mixtures, containing 1.0 mg/ml of liver microsomal protein and 10 μM **1** in 0.1 M phosphate buffer (pH 7.4) were pre-incubated for 5 minutes at 37°C. The reaction was initiated by adding NADPH to a final concentration of 1 mM and the reaction mixtures (final volume 150 μl) were incubated for 60 minutes at 37°C. Control incubations were conducted in the absence of NADPH and in the absence of substrate. The reactions were quenched by adding 150 μl ice-cold acetonitrile. The samples were vortexed for 10 seconds and then centrifuged for 10 minutes at +4°C, 4000 rpm (~ 2750g). The supernatants were stored at -18°C until analysis. 7-ethoxyresorufin was included as a control substrate to confirm CYP1A(1) activity and to get a measurement of EROD activity (Burke et al., 1985). The EROD activity was approximately two times higher in the rat liver microsomes from 3-methylcholanthrene treated rats than in the non-induced rat liver microsomes.

The EC-ESI/MS system. The EC-ESI/MS system was setup as previously reported (Johansson et al., 2007). In short, samples were infused through an ESA Coulochem 5011 analytical cell (ESA Inc., Bedford, MA, USA) via a syringe pump at a flow rate of 5 μl/min. A make-up flow, consisting of 50% methanol and 50% 10 mM aqueous formic acid, was added before the electrochemical cell at a flow rate of 50 μl/min. The electrochemical cell was controlled by an ESA Coulochem II potentiostat (ESA Inc., Bedford, MA, USA). The ESA working electrode was porous graphite and all reported cell potentials were measured versus a palladium reference electrode. The outlet from the ESA cell was connected to a Sciex API 4000 QTrap mass spectrometer (Sciex, Toronto, Canada) equipped with a TurboIonSpray interface. Full scan spectra were acquired continuously.

General electrochemical reaction conditions. The samples were infused through the electrochemical cell at a desired, fixed potential and were collected in glass vials. For electrochemical oxidation followed by LC-MS analysis the substrate concentration in the syringe was 10 μM. For electrochemical synthesis for characterization by NMR the concentration in the syringe was 1 mM. Amodiaquine **1** and desethylamodiaquine **2** were dissolved in methanol.

Electrochemical synthesis for characterization by LC-MS. The amodiaquine aldehyde **3** was generated by infusion of amodiaquine **1** or desethylamodiaquine **2** (10 μM) through the electrochemical cell at a total flow of 55 μl/min (5 μl/min from the syringe and 50 μl/min from the make-up flow). The potential of the first cell (E1) was maintained at +1000 mV and the potential of the second cell (E2) was maintained at -100 mV. In the first cell **1** or **2** was oxidized to the aldehyde but also to the corresponding quinoneimine. In order to enhance the yields of the desired aldehyde product **3** the second cell was set to reduce the quinoneimine byproducts back to aminophenols. The samples were collected for 10 minutes and were stored at -18°C until analysis.

Methoxyl amine adducts were generated by infusion of **1** or **2** (10 μM) through the electrochemical cell at a flow of 55 μl/min for 5 min with the potential of E1 maintained at +1000 mV and the potential of E2 at -100 mV. The oxidized sample was collected in a vial containing methoxyl amine (dissolved in water) to give a final concentration of 5 mM. In order to trap the quinoneimines, **1** or **2** (10 μM) was infused through the electrochemical cell at a flow of 55 μl/min for 5 min with the potential of E1 and E2 maintained at +1000 mV. The oxidized sample was collected in a vial containing *N*-acetyl cysteine (dissolved in water) to give a final concentration of 5 mM. After collection, the samples from the trapping experiments were kept at 25°C for 1 hour before analysis by LC-MS.

Electrochemical synthesis for characterization by NMR. For electrochemical synthesis of amodiaquine aldehyde **3**, amodiaquine **1** (1 mM) was infused through the electrochemical cell at a total flow of 11 μl/min (1 μl/min from the syringe and 10 μl/min from the make-up flow) for approximately

65 h with the potential of E1 maintained at +1500 mV and the potential of E2 at -200 mV. The oxidized sample was collected in an ice-cooled conical glass flask. The sample was kept on ice and the methanol was removed under a stream of nitrogen gas. The remaining water was then removed by lyophilization and the dry residue was kept at -18 °C until analysis by NMR.

LC-MS-SPE-NMR. The sample derived from the electrochemical synthesis was dissolved in approximately 500 μl acetonitrile/water (50:50). Separation was performed using an Agilent 1100 series HPLC system and an Agilent Zorbax (150 x 4.6 mm, 5 μm) column, at a flow rate of 1 ml/min. Mobile phase A consisted of 0.1% formic acid in water and mobile phase B consisted of 0.1% formic acid in acetonitrile. At the start of the gradient, the acetonitrile content was 10% and was linearly increased to 55% over a period of 10 minutes. The acetonitrile content was then increased to 100% within 2 minutes. The initial mobile phase composition was then restored within 0.1 minutes and this condition was held for the remaining 2 minutes. 5% of the flow was diverted to a Bruker Esquire 3000 Mass Spectrometer (Bremen, Germany) for acquisition of full scan MS spectra. Remaining 95% of the flow passed a Bruker UV DAD detector (Coventry, UK) and a make-up flow of 3 ml/min (consisted of 0.1% NH_3 in water) was added to enable trapping on Waters Oasis HLB SPE cartridges (10 x 1mm) using a Spark Prospect 2 system (Emmen, The Netherlands). The trapping was triggered by the MS signal of **3**. For the final NMR sample 5 injections of 40 μl each were trapped on one cartridge. In addition, cleaning of the sample vessel resulted in 300 μl (3x100 μl) diluted sample and this was trapped on a second cartridge. After trapping, the cartridges were dried with nitrogen gas and pooled into one sample by elution with 30 μl deuterated acetonitrile into a 2 mm Bruker Match NMR tube. NMR experiments were performed at 25°C on a Bruker Avance 600 MHz spectrometer (Bremen, Germany) equipped with a 5 mm TCI cryo probe.

LC-MS method. The samples were analysed by liquid chromatography (Waters ACQUITY UPLC, Milford, MA, USA), on a Waters Acquity UPLC BEH (C18 2.1 x 50 mm, 1.7 μm) column, at a flow

rate of 750 μL/min (the column temperature was set at 40°C). Mobile phase A consisted of 5% acetonitrile and 0.1% formic acid in water and mobile phase B was 100% acetonitrile. At the start of the gradient, the acetonitrile content was 1% and was linearly increased to 50% over a period of 5 minutes. The acetonitrile content was then increased to 90% within 0.01 minutes. This condition was held for 0.69 minutes, and finally the initial mobile phase composition was restored within 0.01 minutes. The UPLC system was coupled to a Waters Q-TOF Premier instrument (Wythenshawe, UK) equipped with an electrospray ionization (ESI) source. Leucine-enkephalin was used as the lock mass (*m/z* 556.2771) for accurate mass calibration and introduced using the Lock Spray interface at 20 µL/min (500 pg/μL). All samples were diluted 1:2 in mobile phase A and aliquots of 5 μl were injected onto the LC-MS system. Full scan spectra were acquired in the positive ionisation mode. For acquisition of MS/MS spectra the injection volume was 20 μL and a collision energy ramp (10-30 eV) was used. The softwares used to process the data were MassLynx (version 4.1) and MetaboLynx (Waters). The mass-to-charge ratios of all relevant ions in the MS mode were determined within 5 ppm from the exact mass of the proposed structure. Separate product ion spectrum was acquired for the ^{35}Cl and the ^{37}Cl isotopologues of the aldehyde metabolite **3** to establish whether fragment ions retained the chlorine atom or not.

Results

In the work by Li et al. an unidentified metabolite of amodiaquine (M2) with a pseudomolecular ion (MH^+) at *m/z* 299, was described (Li et al., 2002). This metabolite was formed via the recombinant enzymes CYP1A1 and CYP1B1 but was not observed in human liver microsomes. In the present study the electrochemical experiments with amodiaquine and desethylamodiaquine displayed an oxidation product (oxidation of **1** at +1000 mV followed by reduction at -100 mV) that gave a pseudomolecular ion at *m/z* 299 and eluted at 1.76 min. For comparison of the electrochemically generated oxidation product with the earlier described unidentified metabolite M2, incubations with rCYP1A1, rCYP1B1 were performed. The other rCYPs used in the study by Li et al. were not included in this present study

since metabolite M2 was not formed via these rCYPs. From the corresponding retention times, accurate mass and product ion spectra, the oxidation product from the electrochemical system was shown to be identical with the major metabolite formed by the rCYPs. This metabolite was the same as the unidentified metabolite M2 from the work by Li et al. since it had a pseudomolecular ion at *m/z* 299, a long retention time compared to **1** and was the major metabolite formed via rCYP1A1 and rCYP1B1. From now on this metabolite is referred to as metabolite **3**. Incubations were also conducted with another recombinant CYP450, rCYP2J2. In humans CYP2J2 is mostly found in cardiovascular tissues but is also expressed in human monocytic leukocytes (Nakayama et al., 2008). Metabolite **3** was not formed in these incubations. Metabolite **3** was not seen in the control incubations without NADPH, which suggests a NADPH dependent oxidation of amodiaquine to metabolite **3.** A high energy product ion spectrum of the ^{35}Cl isotopologue of **3** is shown in Fig. 2. Proposed fragmentation pathways are available in the supplemental data.

The accurate mass and product ion spectrum indicate that the structure of **3** corresponds to that of an aldehyde. To test this hypothesis, trapping experiments were performed with *N*-acetyl lysine and methoxyl amine. Trapping with *N*-acetyl lysine did not give any adducts which may be explained by the protonation of *N*-acetyl lysine making it less suitable as a trapping agent at pH 7.4. When methoxyl amine was added to the electrochemical oxidation mixtures and the enzyme incubation mixtures the pseudomolecular ion at *m/z* 299 completely disappeared whereas a new pseudomolecular ion at *m/z* 328 appeared at a retention time shifted about 0.8 minutes in the chromatograms. This pseudomolecular ion corresponds to an addition of 29 Da to **3**, implying that addition of methoxyl amine to the aldehyde had taken place. The product ion spectrum shows an abundant fragment at *m/z* 296, which corresponds to a loss of methanol (32 Da) from *m/z* 328. The product ion spectrum of this methoxyl amine adduct **5** is available in the supplemental data. The methoxyl amine adduct was formed in the incubations with rCYP1A1 and rCYP1B1 but not in the incubations with rCYP2J. This is consistent with the fact that **3** was only formed in the incubations with rCYP1A1 and rCYP1B1. The methoxyl amine adduct was also formed when methoxylamine was added to the electrochemically oxidized samples whereas no adducts

were formed when methoxyl amine was added to untreated samples. When the same trapping experiments were repeated with desethylamodiaquine the same methoxyl amine adduct was formed as in the experiment with amodiaquine. Noteworthy is that desethylamodiaquine and the methoxyl amine adduct of **3** both gave pseudomolecular ions at *m/z* 328, but they were easily distinguished based on their accurate mass and retention times.

The electrochemical oxidation of **1** to **3** was performed on a larger scale in order to synthesize enough material for characterization by NMR. LC-MS-SPE-NMR was performed and the isolated aldehyde **3** was dissolved in deuterated acetonitrile. The sample showed a pure compound with 11 signals in the aromatic region including an OH and an NH signal. 1D ^{1}H-NMR, 1D-NOE experiments as well as COSY and ^{1}H-^{13}C correlated HSQC experiments were performed and chemical shifts were compared to a reference sample of **1** obtained by trapping on the LC-MS-SPE system using the same procedure as described above. From the NMR information it was evident that **3** lacks signals from the ethyl group and the CH_2 group connected to the phenol group in **1**. The ^{1}H and ^{13}C chemical shifts and coupling pattern from the chloroquinolin group were almost identical in **1** and **3** indicating that this part of the molecule is unmodified in **3**. A singlet in the proton spectrum at 9.97 ppm directly bonded to a carbon at 197.0 ppm was a clear indication of an aldehyde group. A NOE was observed between this singlet and a doublet at 7.71 ppm. This doublet showed a small coupling typical for aromatic meta coupling and was assigned to CH(10) according to the numbering in Fig. 3. Thus, comparison of chemical shifts between **3** and **1** and NOE information confirm that the structure of **3** is in accordance with the proposed aldehyde. The ^{1}H-NMR spectrum of **3** along with the structure is shown in Fig. 3. Additional NMR spectra and chemical shifts for **3** and **1** are available in the supplemental data.

It has been previously shown that the quinoneimine metabolite of **1** can be trapped by glutathione or cysteine (Jewell et al., 1995; Lohmann and Karst, 2007; Jurva et al., 2008). Incubations and electrochemical experiments were performed to elucidate whether quinoneimine species were formed in the same systems as the aldehyde metabolite. For these experiments *N*-acetyl cysteine was used as the trapping agent. In the incubations of **1** together with *N*-acetyl cysteine in rCYP1A1 and

rCYP1B1 two new compounds with pseudomolecular ions at *m/z* 460 appeared in the chromatograms. The fact that these two compounds did not form in the incubations with rCYP2J2 indicates that the new compounds originate from the aldehyde species **3**. Successful trapping with *N*-acetyl cysteine implies that the intermediate may be of quinoneimine nature. The proposed structures of the adducts (**6** and **7**), with numbering in the aromatic ring of interest, are shown in Fig. 4. The two chromatographically well separated compounds with the same accurate mass suggests conjugation with *N*-acetyl cysteine in two different positions of the aromatic ring of the aminophenol moiety. Due to a higher steric hindrance in position 2 of the aromatic ring, *N*-acetyl cysteine conjugation at positions 5 and 6 seems to be more probable. The product ion spectra were dominated by a loss of 129 Da, resulting from a cleavage of the thioether on *N*-acetyl cysteine. The product ion spectra of **6** and **7,** together with proposed mechanism for the loss of 129 Da, are shown in the supplemental data. The experiments were repeated with **2** and the same adducts were formed as in the experiments with **1**. The same adducts were also formed with the electrochemical system. The observed metabolism mediated by CYP1A1 and CYP1B1, involving the aldehyde moiety, is shown in Fig. 4. The adducts formed in the trapping experiments are also included in the same figure.

In addition to the *N*-acetyl cysteine adducts of the quinoneimine species of the aldehyde **3**, the quinoneimines of **1** and **2** were also trapped with *N*-acetyl cysteine giving the expected adducts with pseudomolecular ions at *m/z* 517 and *m/z* 489, respectively. These two adducts were observed in rCYP1A1, rCYP1B1 and rCYP2J2, and have not been previously shown in rCYPs. Both the product ion spectra revealed a loss of 129 Da, the same as observed for the *N*-acetyl cysteine adducts above. In addition, a loss of diethylamine (73 Da) from 517 and a loss of ethylamine (45 Da) from 489 were observed. The product ion spectra of the *N*-acetyl cysteine adducts of **1** and **2** formed in the rCYPs are shown in the supplemental data.

In addition to the aldehyde metabolite **3,** three other, to our knowledge not previously reported metabolites (**8**-**10**) of amodiaquine **1** and desethylamodiaquine **2** were discovered in incubations with the rCYPs. These metabolites appeared in incubations with rCYP1A1 and rCYP1B1 but were not

DMD Fast Forward. Published on December 15, 2008 as DOI: 10.1124/dmd.108.025171

formed by rCYP2J2. Metabolite **8** gave a pseudomolecular ion at *m/z* 301 and eluted at 1.38 min. The product ion spectrum is dominated by a fragment at *m/z* 283, which corresponds to a loss of water. The proposed structure is a benzylic alcohol as shown in Fig. 5. Metabolite **9** gave a pseudomolecular ion at *m/z* 315 and eluted at 1.66 min. The product ion spectrum shows a fragment at *m/z* 285, which corresponds to a loss of formaldehyde (30 Da). This is in agreement with the fragmentation pattern of the aldehyde metabolite **3**. Since *m/z* 315 corresponds to an addition of 16 Da to the aldehyde (*m/z* 299) and the product ion spectrum indicates a loss of formaldehyde, metabolite **9** was tentatively assigned as the aldehyde with an additional aromatic hydroxylation as shown in Fig. 5. Metabolite **10** gave a pseudomolecular ion at *m/z* 317 and eluted at 1.21 min. The product ion spectrum of **10** is dominated by a fragment at *m/z* 299, which corresponds to a loss of water. Thus, metabolite **10** was tentatively assigned as the benzylic alcohol (**8**) with an additional aromatic hydroxylation. Interpretation of the product ion spectra of metabolites **9** and **10** indicated that the hydroxylation occurred in the quinoline moiety. Proposed structures of metabolites **8**-**10** are shown in Fig. 5 and product ion spectra of metabolites **8**-**10** are available in the supplemental data. Table 1 shows relative quantities of parent (**1** or **2**, respectively) and metabolites formed by rCYP1A1 and rCYP1B1 after incubation for 30 min as evaluated from the peak areas of the extracted ion chromatograms.

Incubations with **1** in human and rat liver microsomes were performed. Low levels of the aldehyde **3** was formed in both human and rat liver microsomes. The identification was made by comparing the retention times and the product ion spectra with those from the electrochemical standard and the rCYPs. Incubations of **1** with liver microsomes from 3-methylcholanthrene-induced rats and non-induced rats were performed. This was done in order to elucidate whether larger amounts of **3** was formed in the liver microsomes from 3-methylcholanthrene-induced rats compared to non-induced rat liver microsomes, since 3-methylcholanthrene is a known inducer of CYP1A1 and CYP1B1. Extracted ion chromatograms of metabolite **3** formed from amodiaquine via rCYP1A1, rCYP1B1, induced RLM, non-induced RLM and HLM compared to the standard generated electrochemically are presented in Fig. 6. A rough estimation (based on duplicate incubations) of the contribution of the aldehyde to the total

metabolism gave a 6-fold increase of formed aldehyde in the liver microsomes from 3-methylcholanthrene-induced rats compared to the non-induced rat liver microsomes. Trace amounts of the metabolites **8**-**10** were formed in the liver microsomes from 3-methylcholanthrene-induced rats. Trace amounts of metabolite **8** was formed in the non-induced rat liver microsomes, but metabolites **9** and **10** were not observed. Neither of these three metabolites (**8**-**10**) were observed in human liver microsomes.

An unknown metabolite with a pseudomolecular ion at *m/z* 372 appeared in the incubations with rat liver microsomes but was not observed in the incubations with human liver microsomes. This metabolite may have been formed via hydroxylation or *N*-oxidation since the mass corresponds to an addition of 16 Da to amodiaquine. The product ion spectrum, shown in the supplemental data, displays one single fragment at *m/z* 283. Since *m/z* 283 results from a loss of the diethylamine from amodiaquine, this suggests that the oxidation has taken place on the diethylamine part of the molecule. Based on this and the fact that the retention time of the metabolite was 0.23 minutes longer than that of amodiaquine, the structure of the metabolite formed in rat liver microsomes was tentatively assigned as an *N*-oxide on the tertiary amine. The different metabolites contribution to the total metabolism and percentage parent remaining after incubation in liver microsomes for 60 min. are shown in Table 2.

Discussion

This study has shown that the aldehyde metabolite **3** was formed in rCYP1A1, rCYP1B1, human liver microsomes, non-induced rat liver microsomes, rat liver microsomes from 3-methylcholanthrene-induced rats and generated electrochemically. The aldehyde was the major metabolite in rCYP1A1 and rCYP1B1 but was formed only in small amounts in human and rat liver microsomes. This may be explained by the fact that CYP1A1 and CYP1B1 are mainly extrahepatic enzymes that are expressed in the liver only to a small extent. Thus, these CYPs might have a larger impact on extrahepatic metabolism e.g. in the white blood cells than on the metabolism in the liver. CYP1A1 might also play a part in the hepatic metabolism in case of induction, since CYP1A1 is a known subject for induction in

human and in the rat (Bowen et al., 2000; Caron et al., 2005). Human monocytic leukocytes express CYP2J2 (Nakayama et al., 2008) and one severe toxicity of amodiaquine is agranulocytosis. Thus, it was of interest to perform incubations in order to find out if the aldehyde is formed by rCYP2J2. Since the aldehyde was not observed in the incubations with rCYP2J2 no further experiments were performed.

In the study by Li et al. the aldehyde metabolite **3** (in that study referred to as the unidentified metabolite M2) was not observed in incubations with human liver microsomes (Li et al., 2002). In the present study small amounts of **3** was observed in human liver microsomes which may be explained by our slightly different experimental conditions, e.g. higher protein concentration, longer incubation time and a much more sensitive method for analysis compared to the former study.

Previously the group of Park studied the metabolism of **1** in the rat. Three metabolites were described, and designated M4, M5 and M6. M6 was assigned to be a carboxylic acid, whereas M4 and M5 were not identified (Jewell et al., 1995). The new metabolites observed in this present study may correspond to one or more of metabolites M4-M6 proposed in the former study. In addition, the formation of a carboxylic acid metabolite in vivo may further support the in vitro findings of the aldehyde in the present study. Aldehydes are rarely seen in vivo since further oxidation to corresponding carboxylic acids is frequent.

Metabolites **9** and **10** are proposed to be formed by aromatic hydroxylation of **3** and **8**, respectively, rather than via *N*-oxygenation. This hypothesis is based on the observation that **9** behaves as being more polar than **3** and **10** as being more polar than **8** based on their chromatographic retention times as shown in Table 1. This is a common observation under the acidic chromatographic conditions used in this study, as the pK_a of the protonated amine is significantly higher than that of the corresponding N-oxide. Thus the N-oxide would behave chromatographically as being more lipophilic whereas the hydroxylated metabolite would be expected to behave as more polar than the respective parent metabolite. Furthermore, in a previous study of **1** in man the major metabolite besides **2** was tentatively identified as 2-hydroxydesethylamodiaquine by ^{1}H-NMR (Churchill et al., 1985). This further strengthens the proposal that metabolite **9** and metabolite **10** are formed via aromatic

hydroxylation (in the chloroquinoline moiety) of **3** and **8**, respectively. The metabolite with a pseudomolecular ion at *m/z* 372, observed only in the incubations with rat liver microsomes, was tentatively assigned as an *N*-oxide of the tertiary amine moiety of amodiaquine. This is in accordance with the discussion above since the metabolite had a longer retention time, thus behaving as being more lipophilic, than the parent.

As described, all experiments - the incubations as well as the electrochemical experiments - were repeated with **2** and the same metabolites and adducts were formed as when the experiments were performed with **1**. This may be important from a therapeutic point of view as desethylamodiaquine is the major metabolite of amodiaquine in vivo and since the half-life of desethylamodiaquine is significantly longer than that of amodiaquine.

Both desethylamodiaquine and the aldehyde are formed via metabolic *N*-dealkylation. Mechanistically *N*-dealkylations may proceed via hydroxylation at the α-carbon to form a carbinolamine that will spontaneously degrade to the aldehyde and amine, or undergo dehydrogenation to an iminium ion. An equilibrium exists between the carbinolamine and the iminium ion and a general discussion on the *N*-dealkylation of tertiary amines has been published previously (Rose and Castagnoli, 1983).

This study presents the utility of electrochemistry in generating the same oxidation products as those formed by different in vitro systems and, after repeating the oxidation on a larger scale, synthesizing enough material for characterization by NMR. Electrochemical generation of metabolites is a facile method, easy to set up and it usually results in relatively clean product mixtures without many byproducts. An alternative for metabolite generation would be to perform very large liver microsome incubations and separate the metabolite of interest from other formed metabolites and the biological matrix. The disadvantages of this method compared to the electrochemical system are the greater expense, the complex matrix and that optimizing for a certain metabolite would be difficult. In the present study the flow through the electrochemical cell was kept quite low in order to get a high yield of the aldehyde product. The use of a preparative electrochemical cell would further speed up the product

formation because such a preparative cell would be able to handle higher concentrations and thus produce a higher yield of product per time unit.

In conclusion, this study has demonstrated novel metabolic pathways of amodiaquine. Other metabolites were formed via CYP1A1 and CYP1B1 in comparison with those previously reported to be formed in liver microsome incubations. These enzymes, CYP1A1 and CYP1B1, are mainly expressed in extrahepatic tissues e.g. in human leukocytes rather than in the liver. This may be of interest as one of the severe toxicities of amodiaquine treatment is agranulocytosis. Metabolites of particular interest might be the aldehyde metabolite **3** and the aldehyde quinoneimine **4**. Further studies are needed to elucidate whether these metabolites contribute to the amodiaquine toxicity in vivo.

DMD Fast Forward. Published on December 15, 2008 as DOI: 10.1124/dmd.108.025171

Acknowledgements

Roslyn Thelingwani is gratefully acknowledged for help with incubations. Also gratefully acknowledged is Ingvar Nilsson assisting in the lyophilization process of collected sample fractions.

References

Bowen WP, Carey JE, Miah A, McMurray HF, Munday PW, James RS, Coleman RA and Brown AM (2000) Measurement of Cytochrome P450 Gene Induction in Human Hepatocytes using Quantitative Real-Time Reverse Transcriptase-Polymerase Chain Reaction. *Drug Metab Dispos* **28:**781-788.

Burke MD, Thompson S, Elcombe CR, Halpert J, Haaparanta T and Mayer RT (1985) Ethoxy-, pentoxy- and benzyloxyphenoxazones and homologues: a series of substrates to distinguish between different induced cytochromes P-450. *Biochem Pharmacol* **34:**3337-3345.

Caron E, Rioux N, Nicolas O and Lebel-Talbot H (2005) Quantification of the Expression and Inducibility of 12 Rat Cytochrome P450 Isoforms by Quantitative RT-PCR. *J Biochem Mol Toxicol* **19:**368-378.

Christie G, Breckenridge AM and Park BK (1989) Drug-protein conjugates-XVIII. Detection of antibodies towards the antimalarial amodiaquine and its quinone imine metabolite in man and the rat. *Biochem Pharmacol* **38:**1451-1458.

Churchill FC, Patchen LC, Campbell CC, Schwartz IK, D. PN and Dickinson CM (1985) Amodiaquine as a prodrug: importance of metabolite(s) in the antimalarial effect of amodiaquine in humans. *Life Sci* **36:**53-62.

Clarke JB, Maggs JL, Kitteringham NR and Park BK (1990) Immunogenicity of amodiaquine in the rat. *Int Arch Allergy Immunol* **91:**335-342.

Clarke JB, Neftel K, Kitteringham NR and Park BK (1991) Detection of antidrug IgG antibodies in patients with adverse drug reactions to amodiaquine. *Int Arch Allergy Immunol* **95:**369-375.

Durrani N, Leslie T, Rahim S, Graham K, Ahmad F and Rowland M (2005) Efficacy of combination therapy with artesunate plus amodiaquine compared to monotherapy with chloroquine, amodiaquine or sulfadoxine-pyrimethamine for treatment of uncomplicated Plasmodium falciparum in Afghanistan. *Trop Med Int Health* **10:**521-529.

Hakkola J, Pasanen M, Pelkonen O, Hukkanen J, Evisalmi S, Anttila S, Rane A, Mantyla M, Purkunen R, Saarikoski S, Tooming M and Raunio H (1997) Expression of CYP1B1 in human adult and fetal tissues and differential inducibility of CYP1B1 and CYP1A1 by Ah receptor ligands in human placenta and cultured cells. *Carcinogenesis* **18:**391-397.

Harrigan JA, McGarrigle BP, Sutter TR and Olson JR (2006) Tissue specific induction of cytochrome P450 (CYP) 1A1 and 1B1 in rat liver and lung following in vitro (tissue slice) and in vivo exposure to benzo(a)pyrene. *Toxicol in Vitro* **20:**426-438.

Harrison AC, Maggs JL, Kitteringham NR and Park BK (1992) Metabolism and antigenicity of amodiaquine in the rat. *Br J Clin Pharmacol* **33:**212P-213P.

Jewell H, Maggs JL, Harrison AC, O'Neill PM, Ruscoe JE and Park BK (1995) Role of hepatic metabolism in the bioactivition and detoxication of amodiaquine. *Xenobiotica* **25:**199-217.

Johansson T, Weidolf L and Jurva U (2007) Mimicry of phase I drug metabolism - novel methods for metabolite characterization and synthesis. *Rapid Commun Mass Spectrom***:**2323-2331.

Jurva U, Holmén A, Grönberg G, Masimirembwa CM and Weidolf L (2008) Electrochemical Generation of Electrophilic Drug Metabolites: Characterization of Amodiaquine Quinoneimine and Cysteinyl Conjugates by MS, IR, and NMR. *Chem Res Toxicol* **21:**928-935.

Laurent F, Saivin S, Chretien P, Magnaval JF, Peyron F, Sqalli A, Tufenkji AE, Coulais Y and Baba H (1993) Pharmacokinetic and pharmacodynamic study of amodiaquine and its two metabolites after a single oral dose in human volunteers. *Arzneim Forsch* **43:**612-616.

Li XQ, Bjorkman A, Andersson TB, Gustafsson LL and Masimirembwa CM (2003) Identification of human cytochrome P450s that metabolize anti-parasitic drugs and predictions of in vivo drug hepatic clearance from in vitro data. *Eur J Clin Pharmacol* **59:**429-442.

Li XQ, Bjorkman A, Andersson TB, Ridderstrom M and Masimirembwa CM (2002) Amodiaquine clearance and its metabolism to N-desethylamodiaquine is mediated by CYP2C8: A new high affinity and turnover enzyme-specific probe substrate. *J Pharmacol Exp Ther* **300:**399-407.

Lohmann W and Karst U (2007) Generation and Identification of Reactive Metabolites by Electrochemistry and Immobilized Enzymes Coupled On-Line to Liquid Chromatography/Mass Spectrometry. *Anal Chem* **79:**6831-6839.

Madsen KG, Olsen J, Skonberg C, Hansen SH and Jurva U (2007) Development and evaluation of an electrochemical method for studying reactive phase-I metabolites: Correlation to in vitro drug metabolism. *Chem Res Toxicol* **20:**821-831.

Maggs JL, Tingle MD, Kitteringham NR and Park BK (1988) Drug-protein conjugates - XIV. Mechanisms of formation of protein-arylating intermediates from amodiaquine, a myelotoxin and hepatotoxin in man. *Biochem Pharmacol* **37:**303-311.

Mein RM (1951) Camoquin in the treatment of human malaria. *Am J Trop Med Hyg* **31:**212-217.

Mount DL, Patchen LC, D. PN, Barber AM, Schwartz IK and Churchill FC (1986) Sensitive analysis of blood for amodiaquine and three metabolites by high-performance liquid chromatography with electrochemical detection. *J Chromatogr* **383:**375-386.

Naisbitt DJ, Williams DP, O'Neill PM, Maggs JL, Willock DJ, Pirmohamed M and Kevin Park B (1998) Metabolism-dependent neutrophil cytotoxicity of amodiaquine: A comparison with pyronaridine and related antimalarial drugs. *Chem Res Toxicol* **11:**1586-1595.

Nakayama K, Nitto T, Inoue T and Node K (2008) Expression of the cytochrome P450 epoxygenase CYP2J2 in human monocytic leukocytes. *Life Sci* **83:**339-345.

Pushparajah DS, Umachandran M, Nazir T, Plant KE, Plant N, Lewis DFV and Ioannides C (2008) Up-regulation of CYP1A/B in rat lung and liver, and human liver precision-cut slices by a series of polycyclic aromatic hydrocarbons; association with the Ah locus and importance of molecular size. *Toxicol In Vitro* **22:**128-145.

Pussard E, Verdier F, Faurisson F, Scherrmann JM, Le Bras J and Blayo MC (1987) Disposition of monodesethylamodiaquine after a single oral dose of amodiaquine and three regimens for prophylaxis against Plasmodium falciparum malaria. *Eur J Clin Pharmacol* **33:**409-414.

Rose J and Castagnoli N (1983) The metabolism of tertiary amines. *Med Res Rev* **3:**73-88.

Shimada T, Oda Y, Gillam EMJ, Guengerich FP and Inoue K (2001) Metabolic Activation of Polycyclic Aromatic Hydrocarbons and Other Procarcinogens by Cytochromes P450 1A1 and P450 1B1 Allelic Variants and Other Human Cytochromes P450 in Salmonella typhimurium NM2009. *Drug Metab Dispos* **29:**1176-1182.

Stiborova M, Dracinska H, Hajkova J, Kaderabkova P, Frei E, Schmeiser HH, Soucek P, Phillips DH and Arlt VM (2006) The Environmental Pollutant and Carcingen 3-nitrobenzanthrone and its Human Metabolite 3-aminobenzanthrone are Potent Inducers of Rat Hepatic Cytochromes P450 1A1 and -1A2 and NAD(P)H:quinone Oxidoreductase. *Drug Metab Dispos* **34:**1398-1405.

Stiborova M, Martinek V, Rydlova H, Hodek P and Frei E (2002) Sudan I Is a Potential Carcinogen for Humans: Evidence for Its Metabolic Activation and Detoxication by Human Recombinant Cytochrome P450 1A1 and Liver Microsomes. *Cancer Res* **62:**5678-5684.

Stiborova M, Martínek V, Rýdlová H, Koblas T and Hodek P (2005) Expression of cytochrome P450 1A1 and its contribution to oxidation of a potential human carcinogen 1-phenylazo-2-naphthol (Sudan I) in human livers. *Cancer Lett* **220:**145-154.

Zhou F and Van Berkel GJ (1995) Electrochemistry Combined Online with Electrospray Mass Spectrometry. *Anal Chem* **67:**3643-3649.

DMD Fast Forward. Published on December 15, 2008 as DOI: 10.1124/dmd.108.025171

Footnotes

Primary Laboratory of Origin: Discovery DMPK & Bioanalytical Chemistry AstraZeneca R&D, Mölndal

Dr. Collen Masimirembwa was funded by the International Programme in Chemical Sciences (IPICS), Uppsala University, Sweden.

DMD Fast Forward. Published on December 15, 2008 as DOI: 10.1124/dmd.108.025171

Legends for figures

Fig. 1. Molecular structures of amodiaquine **1**, desethylamodiaquine **2**, and the aldehyde **3**.

Fig. 2. Product ion spectrum of the ^{35}Cl isotopologue of the aldehyde metabolite **3**. A collision energy of 40V was used. (Proposed fragmentation pathways are available in the supplemental data).

Fig. 3. ^{1}H-NMR spectra of the aldehyde metabolite **3**.

Fig. 4. Metabolic routes of amodiaquine and desethylamodiaquine observed in rat and human liver microsomes and recombinant CYP1A1 and 1B1. Trapping reactions were performed on metabolites formed in the rCYP incubations. All metabolites and trapped adducts were also obtained in the electrochemical system.

Fig. 5. Proposed structures for amodiaquine metabolites **8**-**10**, formed in incubations with rCYP1A1 and rCYP1B1.

Fig. 6. The aldehyde metabolite **3** formed in incubations with rCYP1A1, rCYP1B1, 3-methylcholanthrene-induced RLM, (non-induced) RLM, HLM and standard generated in the electrochemical system. Extracted ion chromatograms of *m/z* 299. The retention time has shifted slightly compared to the retention time in Table 1 and in the text since the analyses were performed on different occasions. Metabolite **3** was not observed in any of the samples without NADPH.

DMD Fast Forward. Published on December 15, 2008 as DOI: 10.1124/dmd.108.025171

TABLE 1

Relative metabolite amounts of the fraction metabolized of amodiaquine and desethylamodiaquine respectively in liver microsomes incubated for 30 min. Data estimated from integration of extracted ion chromatograms.

			Amodiaquine(%)		Desethylamodiaquine(%)	
Structure	*m/z*	t_R	rCYP1A1	rCYP1B1	rCYP1A1	rCYP1B1
2	328	0.87	3.0	5.3	-	-
3	299	1.76	51	77	59	82
8	301	1.38	24	8.0	19	7.9
9	315	1.66	8.1	9.3	7.8	11
10	317	1.21	14	trace[a]	14	trace[a]
Percentage of amodiaquine remaining after 30min. incubation						
1	356	0.97	32	45	-	-
Percentage of desethylamodiaquine remaining after 30min. incubation						
2	328	0.87	-	-	10	45

[a]trace, trace amounts observed

DMD Fast Forward. Published on December 15, 2008 as DOI: 10.1124/dmd.108.025171

TABLE 2

Relative metabolite amounts of the fraction metabolized of amodiaquine in liver microsomes incubated for 60 min. Data estimated from integration of extracted ion chromatograms. Values shown in the table are averaged numbers from duplicate incubations.

Structure	*m/z*	induced RLM	RLM	HLM
Percentage of metabolites after incubation of **1** for 60 min.				
2	328	74	59	94
3	299	13	2.0	0.2
8	301	trace[a]	trace[a]	-
9	315	trace[a]	-	-
10	317	trace[a]	-	-
N-oxide	372	10	29	-
Other	-	3.5	10	5.5
Percentage of amodiaquine remaining after 60min. incubation				
1	356	70	52	3.1

[a]trace, trace amounts observed

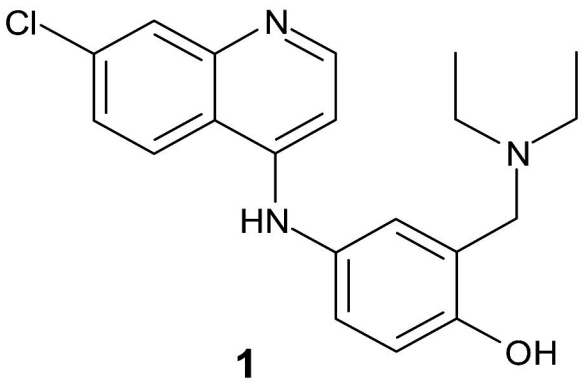

1

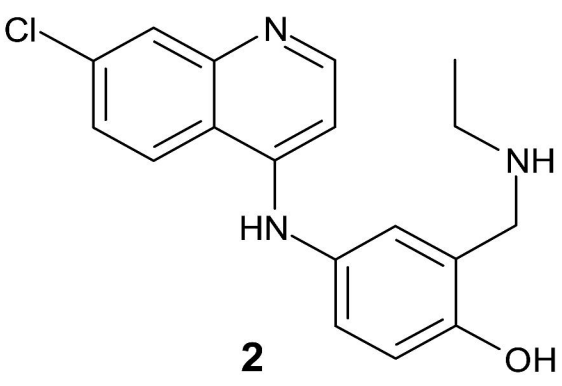

2

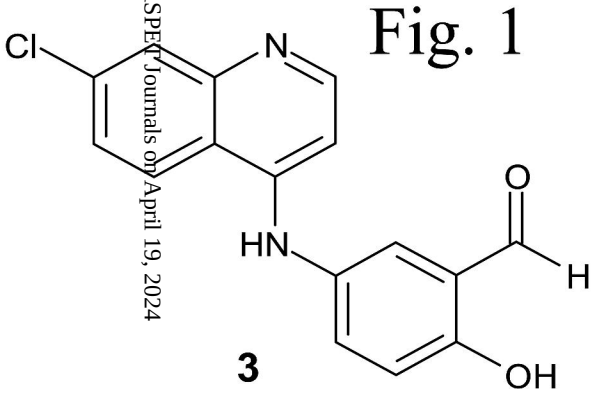

3

Fig. 1

DMD Fast Forward. Published on December 15, 2008 as DOI: 10.1124/dmd.108.025171
This article has not been copyedited and formatted. The final version may differ from this version.

Fig. 2

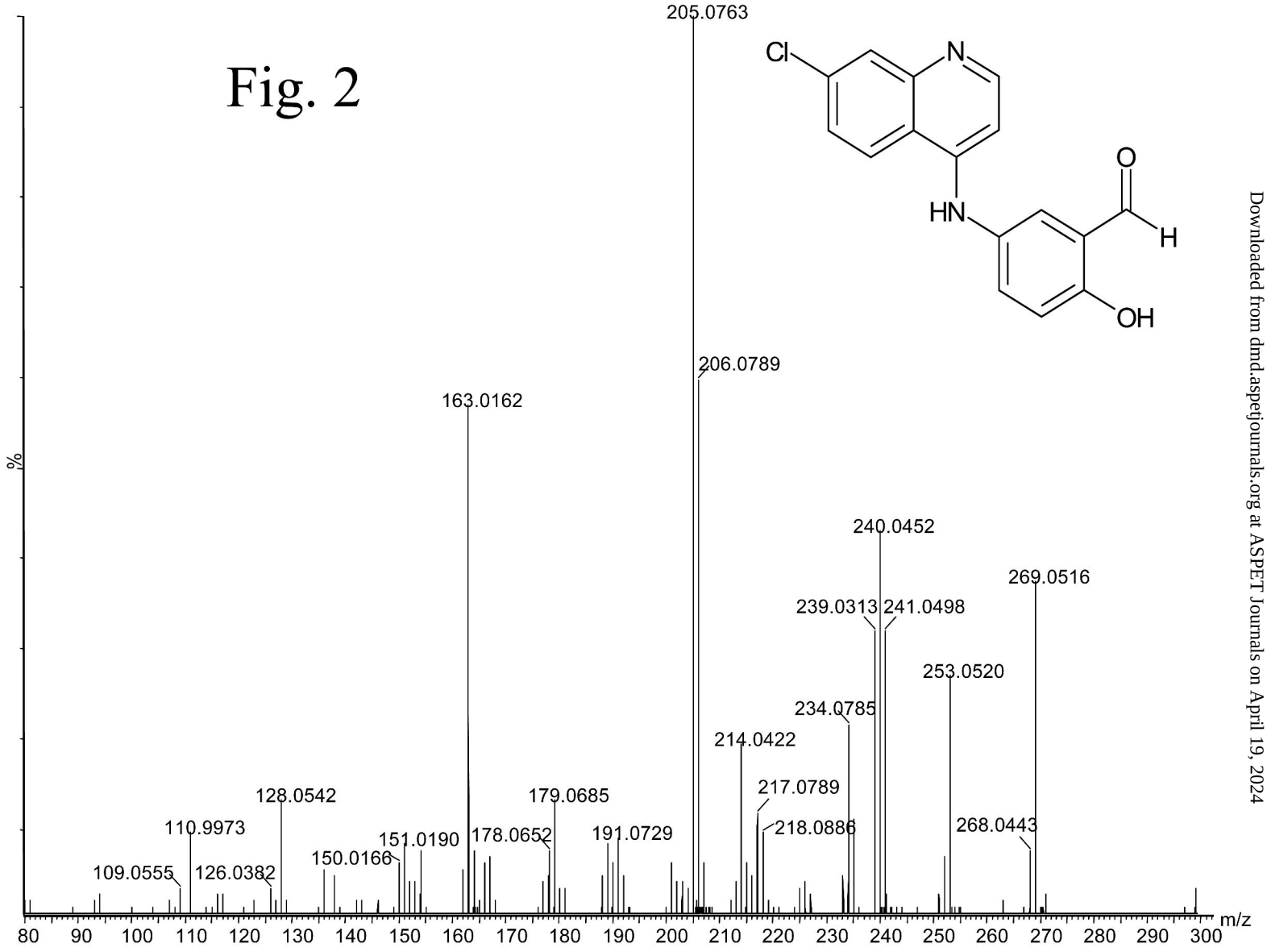

DMD Fast Forward. Published on December 15, 2008 as DOI: 10.1124/dmd.108.025171
This article has not been copyedited and formatted. The final version may differ from this version.

Fig. 3

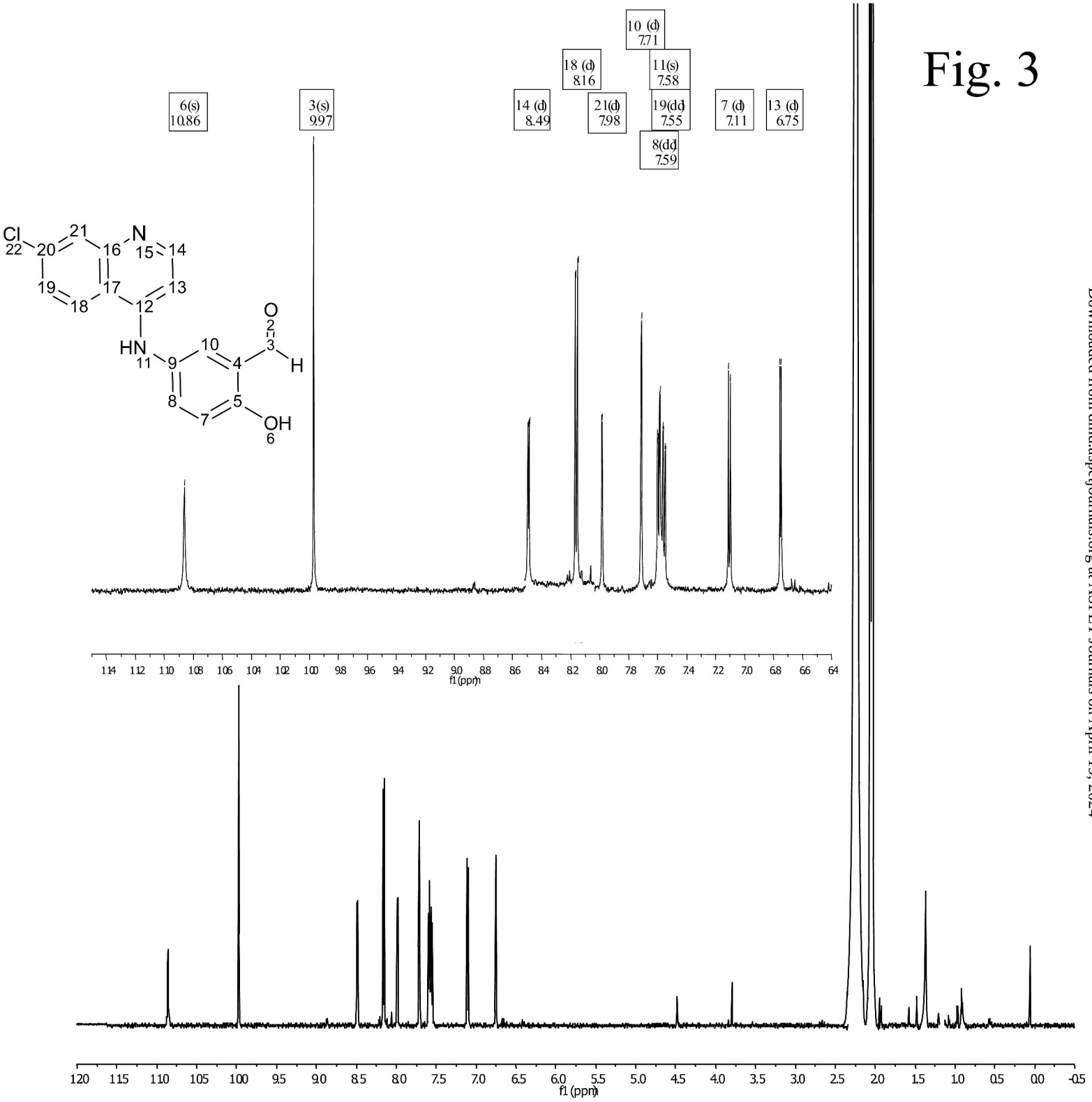

DMD Fast Forward. Published on December 15, 2008 as DOI: 10.1124/dmd.108.025171
This article has not been copyedited and formatted. The final version may differ from this version.

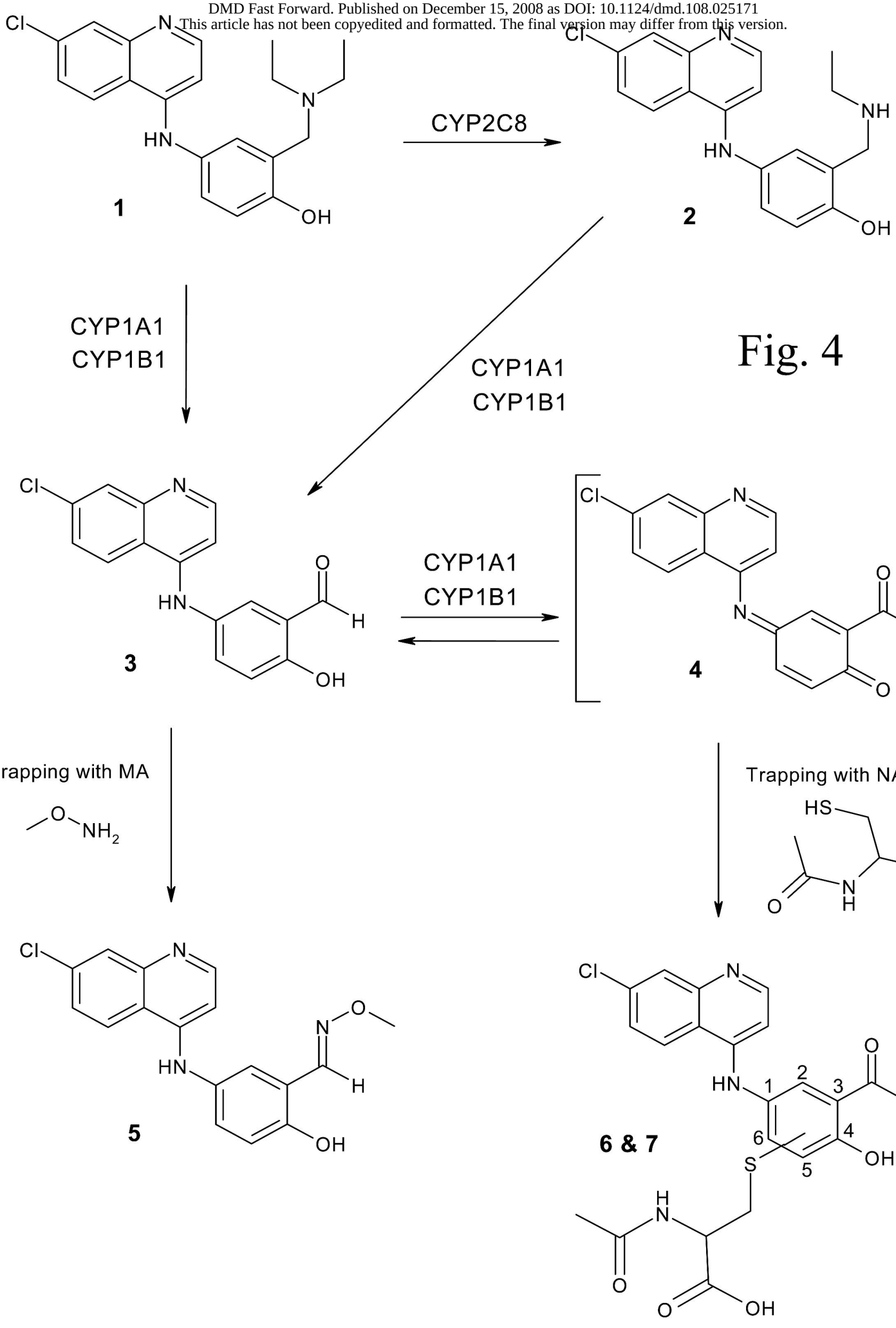

Fig. 4

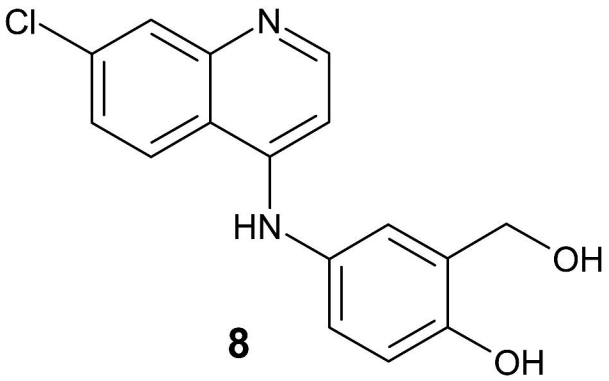

8

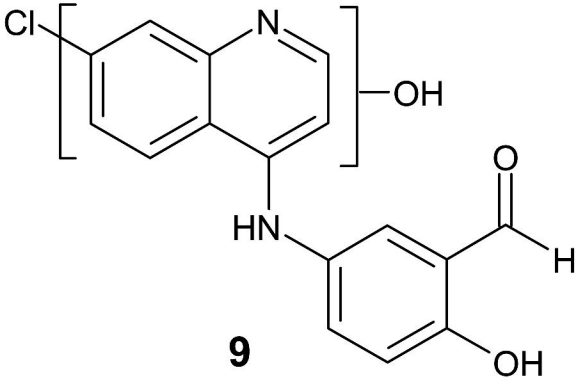

9

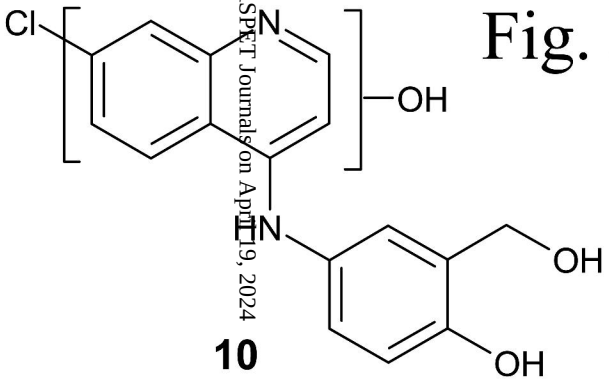

10

Fig. 5

DMD Fast Forward. Published on December 15, 2008 as DOI: 10.1124/dmd.108.025171
This article has not been copyedited and formatted. The final version may differ from this version.

Fig. 6